



Cite this: *New J. Chem.*, 2021, 45, 9864

Regioselectivity of aminomethylation in 3-acetyl-7-hydroxycoumarins: Mannich bases and Betti bases†

Fan Gao, Deng Tao, Cheng Ju, Bei-Bei Yang, Xiu-Qi Bao, Dan Zhang, Tian-Tai Zhang and Li Li *

7-Hydroxycoumarin is a privileged structure for anti-inflammatory drug development. In this study, several new 3-acetyl-7-hydroxycoumarin derivatives were designed, synthesized and tested as anti-inflammatory agents. Interestingly, Mannich bases and Betti bases were separately obtained under acidic or neutral conditions. The regioselectivity of aminomethylation was studied based on the atomic electron density distribution by analysing the Voronoi deformation density (VDD) atomic charges, which reasonably explained the experimental outcome. Detection of nitric oxide (NO) and tumour necrosis factor alpha (TNF- α) release revealed that Mannich bases displayed stronger anti-inflammatory activity than the corresponding Betti bases.

Received 1st April 2021,
Accepted 7th May 2021

DOI: 10.1039/d1nj01584b

rsc.li/njc

Introduction

Inflammation is a protective process that occurs in response to infection or injury. However, persistent inflammation can lead to tissue damage and even severe host injury *via* release of inflammatory mediators.^{1,2} Chronic inflammation is a prominent factor in the pathogenic mechanisms of a wide range of inflammatory conditions and diseases, such as atherosclerosis, rheumatoid arthritis, cancers and Parkinson's disease.^{3–6}

7-Hydroxycoumarin extracted from *Justicia pectoralis* has been reported to possess anti-inflammatory potential.⁷ Compounds containing 7-hydroxycoumarin moieties are ubiquitous in natural fruits and plants and have gained widespread attention due to their biological activities, such as antioxidant and anti-inflammatory activities.^{8,9} Recently, 3-acetyl-7-hydroxycoumarin derivatives have been reported to be macrophage migration inhibitory factor (MIF) tautomerase inhibitors and MIF-CD47 antagonists.^{10,11}

The Mannich aminoalkylation reaction is a three-component condensation reaction that typically occurs among an amine or ammonia, formaldehyde and an α -H atom adjacent to a carbonyl group. This reaction has excellent potential for synthetic and medicinal chemistry^{12–14} and has recently also received considerable attention in pesticide chemistry.¹⁵ Mannich bases are very useful for improving the bioavailability, hydrophilic properties

and chemical stability of drugs.^{16,17} The ketonic Mannich reaction has been applied for industrial fluoxetine and atropine production.^{18,19}

Betti bases, namely, phenolic Mannich bases, represent a special type of Mannich base. They were first synthesized and reported by Mario Betti in the early 20th century.²⁰ Betti bases can be used as asymmetric catalyst ligands,²¹ fluorescent probes,²² and other tools. The ligand AF40431 of the neuronal receptor sortilin (1, Fig. 1) and calcein blue (2) are typical Betti bases displaying biological activities.^{23,24} Moreover, Betti bases 3 and 4 are effective against inflammation.^{25,26}

In our previous work, 3-acetyl-7-hydroxycoumarin Mannich bases (5, Fig. 1) were demonstrated to strongly counteract monoamine oxidase B and neuroinflammation.¹⁷ Interestingly,

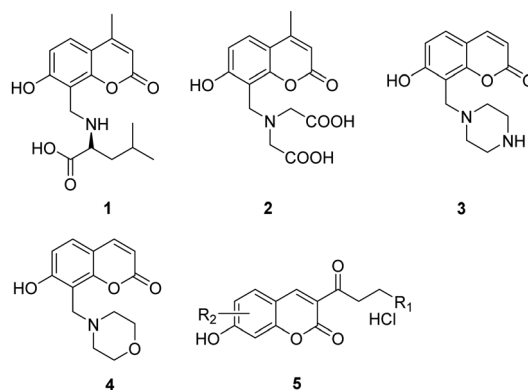


Fig. 1 Representative Betti bases and Mannich bases.

Beijing Key Laboratory of Active Substances Discovery and Druggability Evaluation, Institute of Materia Medica, Chinese Academy of Medical Sciences & Peking Union Medical College, Beijing 100050, China. E-mail: annaleelin@imm.ac.cn

† Electronic supplementary information (ESI) available: ¹H- and ¹³C-NMR, ESI-MS/MS spectra and Cartesian coordinates. See DOI: 10.1039/d1nj01584b

during optimization of the reaction conditions, derivatization occurred at the C8 position or the ketonic methyl group to induce the formation of Betti bases or ketonic Mannich bases, respectively. Electron density distribution is thought to affect regioselectivity. Some density functional theory (DFT) approaches, including electrostatic potential (ESP),²⁷ Voronoi deformation density (VDD)²⁸ charges, average local ionization energy (ALIE),²⁹ the Fukui function³⁰ and a dual descriptor (FDD),³¹ could be adopted to predict this property and determine regioselectivity.

To develop anti-inflammatory coumarin aminoalkylation derivatives, various ketonic Mannich bases and Betti bases were prepared. The underlying factors determining the regioselectivity were investigated by using DFT to calculate the atomic charge distribution. The anti-inflammatory activities of these compounds were assessed by evaluating the inhibitory activity of the compounds against nitric oxide (NO) production and tumour necrosis factor alpha (TNF- α) in mouse macrophages.

Results and discussion

Synthesis

The synthetic routes to target compounds **8–29** are shown in Scheme 1.

Intermediates **6** and **7** were obtained through the Knoevenagel reaction and Pechmann condensation, respectively. The Mannich reaction took place at the α -H of the carbonyl group to yield compounds **8–18** in ethanol under acidic conditions (pH 2–3) with reflux at 78 °C. Only mono-Mannich bases were obtained, even if large excesses of paraformaldehyde (PFA) and secondary amine were added. However, when hydrochloric acid was not added to the reaction mixture of PFA, piperidine and intermediate **6**, an unexpected compound instead of target molecule **8** was detected by using thin-layer chromatography (TLC). The aromatic proton signal ($\delta = 6.8$ ppm) corresponding to H8 was absent from

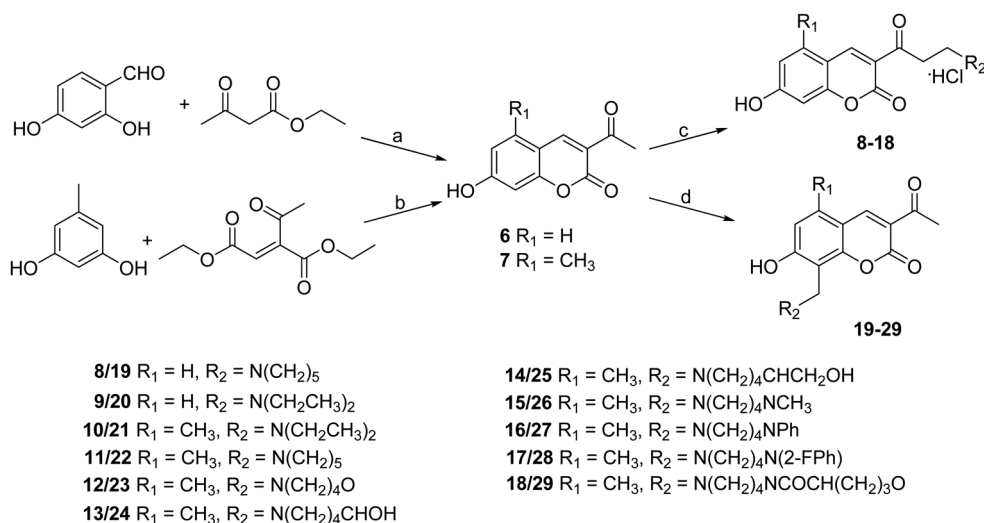
the ¹H-NMR spectrum, indicating that aminomethylation took place at the C8 position. Thus, hydrochloric acid is crucial to regioselectivity. Under the same conditions used for compound **19**, compounds **20–29** were obtained in modest to high yields.

For either the Mannich reaction or the Betti reaction, the first step is to mix PFA and a secondary amine in ethanol. The reactant ratio of the Mannich reaction is ten equivalents of PFA and secondary amine relative to the coumarin intermediate.¹⁵ The optimized ratio for the secondary amine, PFA and the coumarin intermediate in the Betti reaction was 10 : 5 : 1.

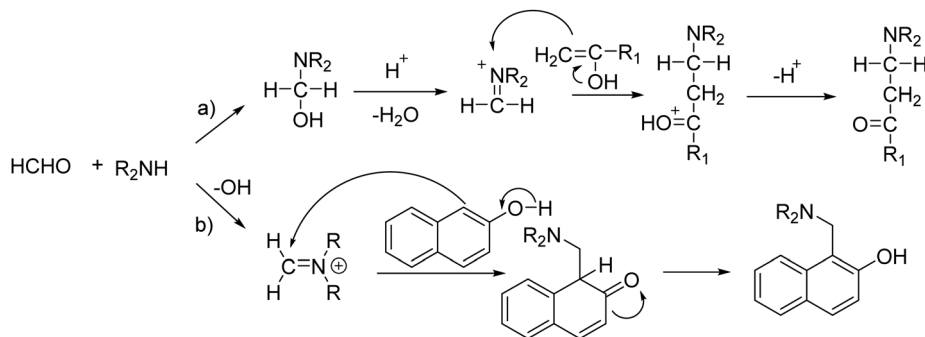
Theoretical interpretation of regioselectivity

The mechanism underlying the Mannich reaction has been explored for decades, but the exact mechanism is still uncertain.^{10,32–34} When additional acid is added, the first step is generally thought to be the formation of an *N*-hydroxymethyl amine intermediate, followed by the removal of water to yield imine cations. Then, the enols (or enolates) serve as nucleophiles in the nucleophilic addition reaction to generate ketonic Mannich bases (Scheme 2a).³² Without acid, the prototypical nucleophile attacks the imine to yield the aminomethylation derivative.^{35,36}

Intermediate **6** was selected for theoretical exploration of regioselectivity using DFT. Atomic charges are the most intuitive and concise representations of charge distribution in chemical systems.³⁷ In principle, atoms with more negative (positive) atomic charges tend to be more favourable sites for attack by nucleophiles (electrophiles).³⁸ Among various approaches to express charge density, VDD charge and Hirshfeld charge approaches can reliably determine regioselectivity and accurately quantify nucleophilicity and electrophilicity.³⁹ The VDD method was employed to analyse electron density distribution in this study. The VDD charge Q_A is computed as the integral of the deformation density $\Delta\rho(r)$ related to the formation of a molecule from atoms within the volume of the so-called Voronoi cell of



Scheme 1 Synthetic routes to target compounds **8–29**. Reagents and conditions: (a) piperidine, CH₃COOH, ethanol, rt, 5 h; (b) C₂H₅ONa, ethanol, reflux, 1.5 h; (c) PFA, secondary amines or heterocyclic amines, ethanol, concentrated hydrochloric acid, reflux, 12 h; (d) PFA, secondary amines or heterocyclic amines, ethanol, reflux, 8 h.



Scheme 2 Reported mechanism of the Mannich reaction catalysed by acids (a) and a plausible mechanism of the process used to obtain Betti base derivatives (b).

atom A (eqn (1)).^{28,40} The Voronoi cell of atom A is designated as the area defined by the bond midplanes on and vertical to all bond axes between nucleus A and its adjacent nuclei.⁴¹

$$Q_A = \int_{\text{Voronoi cell of A}} \left(\rho(r) - \sum_B \rho_B(r) \right) dr \quad (1)$$

To evaluate the applicability of VDD charges for coumarins, the ¹H-NMR spectrum of 7-hydroxycoumarin (**30**) was obtained in methanol-*d*₄. There is a linear correlation between charge density and chemical shifts^{42,43} that reflects the magnetic shielding effects of extranuclear electrons.⁴⁴ The VDD charges of the aromatic carbon atoms in 7-hydroxycoumarin were in line with the corresponding chemical shifts (Fig. 2).

The atomic charges of intermediate **6** were analysed with the VDD method (Fig. 3a). The results showed that C8 was more negatively charged than C5 and C6, making C8 a better site for nucleophilic attack. These data suggest that the Betti reaction took place at C8 instead of at C6 without addition of hydrochloric acid. However, when the reaction solution was acidic (pH 2–3), the 3-acetyl group in compound **6** likely promoted keto–enol tautomerism to enable direct insertion of electrophilic groups at α -C.⁴⁵ The VDD charges on the α -C of the 3-acetyl group were more negative than those on the C8 atom (–0.118 a.u. vs. –0.096 a.u.).

The VDD method was also adopted to analyse the reactivity of three coumarin derivatives, 4-phenyl-7-hydroxycoumarin (**31**, Fig. 3b), 4-methyl-6-hydroxycoumarin (**32**), and 4,7-dimethyl-5-hydroxycoumarin (**33**). It has been reported that the aminomethylation reaction of compound **31** takes place at the C8 position,^{46,47} which bore a negative atomic charge of –0.099 a.u. Compound **32** had a lower charge density on the

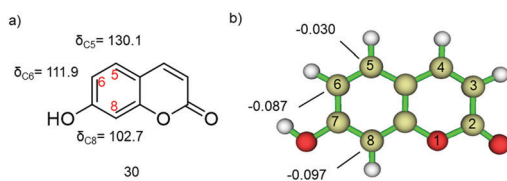


Fig. 2 Comparison of the chemical shifts and VDD charges of aromatic carbon atoms of **30**. (a) Chemical shifts of C5, C6 and C8; (b) Q_A values (a.u.) of C5, C6 and C8.

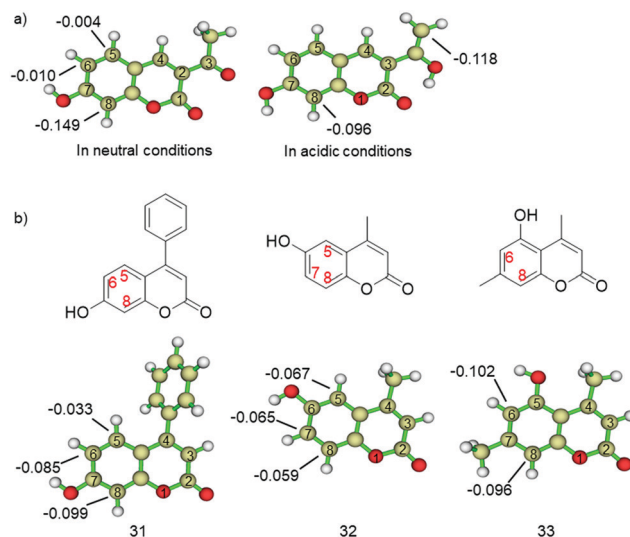


Fig. 3 Calculated VDD charges (Q_A) of compounds **6** and **31–33**. (a) Compound **6**; (b) compounds **31–33**.

phenyl ring (more than –0.07 a.u.), which hindered its reaction.⁴⁸ C6 and C8 on compound **33** displayed similar charge densities, leading to a mixture of products.⁴⁸ Thus, the VDD atomic charge results were all consistent with the chemical experiment results, indicating that charge density analysis is a valuable tool for prediction of the regioselectivity and nucleophilicity of the Mannich reaction for these coumarin analogues.

Anti-inflammatory activity

The anti-inflammatory effects of the target compounds were evaluated by detecting NO release in LPS-induced RAW264.7 mouse macrophages.⁴⁹ Curcumin, a well-known anti-inflammatory natural product, is used as the positive control.^{17,50a} It is the main active ingredient in the spice turmeric and displays various biological activities including anti-inflammatory and anti-cancer activities.⁵⁰

Compounds **13**, **15** and **18** were shown to exhibit good anti-inflammatory activity (Table 1), and the coumarin Mannich bases displayed stronger anti-inflammatory activity than the

Table 1 NO release-inhibiting activity of the target compounds

Compd	Inhibition ratio ^a (%)	Compd	Inhibition ratio ^a (%)
8	26.76	19	4.09
9	47.94	20	3.18
10	57.65	21	1.36
11	56.76	22	7.73
12	13.53	23	-1.07
13	62.27	24	18.13
14	55.91	25	7.73
15	67.35	26	1.33
16	27.73	27	-1.07
17	17.94	28	2.13
18	66.82	29	10.93
		Curcumin	87.11

^a Inhibition of NO production tested at 10 μ M.

coumarin Betti bases. Structure–activity relationship assessment showed that the *N*-methylpiperazine Mannich derivative **15** displayed the highest anti-inflammatory activity. When the methyl group was replaced by phenyl groups (**16**, **17**), the activity decreased dramatically, possibly due to steric hindrance of the phenyl groups. Substitution of 4-hydroxypiperidine as the hydrogen donor also improved the activity. Comparison of the anti-inflammatory activities of compounds **11** and **10** with those of compounds **8** and **9** revealed that the presence of a 5-methyl group on the coumarin ring may contribute to the inhibition of NO production.

In addition, the inhibitory activities of some compounds (**8–11**, **19–22**) against TNF- α release were tested using lipopolysaccharide (LPS)-treated RAW246.7 cells. Compounds **10** and **21** showed moderate activity compared with the positive control dexamethasone (Table 2), indicating that the diethylamino group was beneficial to the anti-inflammatory activity. The Mannich bases displayed obviously stronger anti-inflammatory activity than the corresponding Betti bases in both models.

Conclusions

In conclusion, twenty-two coumarin ketonic Mannich bases and Betti bases were synthesized and tested as anti-inflammatory agents. The regioselectivity on 3-acetyl-7-hydroxycoumarin was studied by using DFT calculations of the atomic charge distribution, and the VDD method was adopted to determine the possible reactive site. The Mannich bases exhibited much stronger anti-inflammatory activity than the corresponding Betti bases in both NO release and TNF- α production models.

Table 2 Inhibitory activities of compounds **8–11** and **19–22** against TNF- α release

Compd	Inhibition ratio ^a (%)	Compd	Inhibition ratio ^a (%)
8	1.35	19	1.78
9	31.03	20	5.37
10	59.34	21	49.13
11	10.51	22	-3.04
	Dexamethasone		70.00

^a Inhibition of TNF- α production tested at 10 μ M.

Materials and methods

Chemistry

Commercially available reagents were purchased from Innochem (Shanghai, China) and used without further purification. With tetramethylsilane (TMS) as an internal standard, ¹H-NMR and ¹³C-NMR spectra were recorded on a Jeol ECZ-400S, a Bruker Avance-III or WNMRI-500, and a Bruker Avance-600 NMR System by using DMSO-*d*₆, D₂O, CDCl₃, CD₃OD and CF₃COOD as deuterated solvents. For compounds **24** and **25**, a small amount of CF₃COOD was added to D₂O to improve solubility. ESI-HRMS data were collected on an Agilent 6520 Accurate-Mass Q-TOF LC/MS spectrometer. TLC was conducted with glass precoated with silica gel GF254 (Qingdao Marine Chemical Inc., China) to monitor the reactions. Melting points were measured with a Yanaco MP-J3 melting point apparatus.

Compounds **6** and **7** were synthesized using the protocol described in our previous report.¹⁷

The general procedure for the preparation of target compounds **8–18** is described below.

A secondary alkyl amine (20.0 mmol, 10 equiv.) was added to a stirred suspension of PFA (0.61 g, 20.0 mmol, 10 equiv.) (Innochem, #A34195) in ethanol (25 mL), and the pH of the solution was adjusted to 2–3 with concentrated hydrochloric acid. After 2 h of reflux at 78 °C, coumarin intermediate **6** or **7** (2.0 mmol, 1 equiv.) was added, and the reaction mixture was refluxed at 78 °C for 10–30 h and monitored with TLC. Subsequently, the mixture was cooled to room temperature and filtered to obtain a yellow solid. The residue was washed three times with ethanol or methanol to obtain a pure product.

3-(3-Piperidyl propionyl)-7-hydroxycoumarin hydrochloride (8). Yellow solid, yield: 80%, m.p.: 244–246 °C (decomposed). The ¹H- and ¹³C-NMR data were identical to those in our previous report.¹⁵ ESI-HRMS: *m/z* [M + H]⁺ calcd for C₁₇H₂₀NO₄ 302.1387, found 302.1378.

3-(3-Diethylamino propionyl)-7-hydroxycoumarin hydrochloride (9). Yellow solid, yield: 77.9%, m.p.: 194–197 °C (decomposed). ¹H-NMR (400 MHz, DMSO-*d*₆): δ 11.41 (br, 1H, D₂O exchangeable), 10.11 (br, 1H, D₂O exchangeable), 8.70 (s, 1H), 7.84 (d, *J* = 8.6 Hz, 1H), 6.91 (dd, *J* = 8.6, 2.2 Hz, 1H), 6.83 (d, *J* = 2.2 Hz, 1H), 3.52 (t, *J* = 7.2 Hz, 2H), 3.35 (t, *J* = 7.2 Hz, 2H), 3.13 (q, *J* = 7.2 Hz, 4H), 1.23 (t, *J* = 7.2 Hz, 6H). ¹³C-NMR (100 MHz, DMSO-*d*₆): δ 193.6, 164.8, 159.0, 157.3, 148.6, 132.9, 118.1, 114.5, 110.7, 101.8, 46.6, 46.1, 36.2, 8.5. ESI-HRMS: *m/z* [M + H]⁺ calcd for C₁₆H₂₀NO₄ 290.1387, found 290.1382.

3-(3-Diethylamino propionyl)-5-methyl-7-hydroxycoumarin hydrochloride (10). Yellow solid, yield: 61.2%, m.p.: 201–203 °C (decomposed). ¹H-NMR (400 MHz, DMSO-*d*₆): δ 11.35 (br, 1H), 10.17 (br, 1H), 8.61 (s, 1H), 6.78 (d, *J* = 2.1 Hz, 1H), 6.68 (d, *J* = 2.1 Hz, 1H), 3.54 (t, *J* = 7.2 Hz, 2H), 3.35 (t, *J* = 7.2 Hz, 2H), 3.13 (q, *J* = 7.2 Hz, 4H), 2.50 (overlapped, 3H), 1.24 (t, *J* = 7.2 Hz, 6H). ¹³C-NMR (100 MHz, DMSO-*d*₆): δ 193.6, 164.5, 158.9, 158.1, 145.2, 141.5, 117.1, 115.5, 109.8, 100.0, 46.6, 46.0, 36.1, 18.0, 8.5. ESI-HRMS: *m/z* [M + H]⁺ calcd for C₁₇H₂₂NO₄ 304.1543, found 304.1548.

3-(3-Piperidyl propionyl)-5-methyl-7-hydroxycoumarin hydrochloride (11). Yellow solid, yield: 84%, m.p.: 227–230 °C

(decomposed). The ^1H - and ^{13}C -NMR data are the same as those in our previous report.¹⁵ ESI-HRMS: m/z $[\text{M} + \text{H}]^+$ calcd for $\text{C}_{18}\text{H}_{22}\text{NO}_4$ 316.1543, found 316.1541.

3-(3-Morpholinyl propionyl)-5-methyl-7-hydroxycoumarin hydrochloride (12). Yellow solid, yield: 86%, m.p.: 239–241 °C (decomposed). The ^1H - and ^{13}C -NMR data are the same as those in our previous report.¹⁷ ESI-HRMS: m/z $[\text{M} + \text{H}]^+$ calcd for $\text{C}_{17}\text{H}_{20}\text{NO}_5$ 318.1336, found 318.1331.

3-(3-(4-Hydroxypiperidin-1-yl)propionyl)-5-methyl-7-hydroxycoumarin hydrochloride (13). Yellow solid, yield: 82.1%, m.p.: 201–203 °C (decomposed). ^1H -NMR (400 MHz, $\text{DMSO}-d_6$): δ 11.32 (br, 1H), 10.12 (br, 1H), 8.61 (s, 1H), 6.77 (dd, $J = 2.2, 0.8$ Hz, 1H), 6.67 (d, $J = 2.2$ Hz, 1H), 3.57–2.98 (m, 9H), 2.50 (overlapped, 3H), 1.99–1.92 (m, 2H), 1.75–1.65 (m, 2H). ^{13}C -NMR (100 MHz, $\text{DMSO}-d_6$): δ 193.6, 164.5, 158.9, 158.1, 145.2, 141.6, 117.1, 115.5, 109.8, 100.0, 64.1, 59.4, 47.3, 31.6, 29.4, 18.0. ESI-HRMS: m/z $[\text{M} + \text{H}]^+$ calcd for $\text{C}_{18}\text{H}_{22}\text{NO}_5$ 332.1492, found 332.1489.

3-(3-(4-(Hydroxymethyl)piperidin-1-yl)propanoyl)-5-methyl-7-hydroxycoumarin hydrochloride (14). Yellow solid, yield: 81.6%, m.p.: 210–211 °C (decomposed). ^1H -NMR (400 MHz, $\text{DMSO}-d_6$): δ 11.37 (br, 1H), 10.03 (br, 1H), 8.60 (s, 1H), 6.77 (d, $J = 2.0$ Hz, 1H), 6.67 (d, $J = 2.0$ Hz, 1H), 3.58 (t, $J = 7.2$ Hz, 2H), 3.47 (d, $J = 12.0$ Hz, 2H), 3.46–3.34 (m, 2H), 3.25 (d, $J = 6.0$ Hz, 2H), 2.96–2.88 (m, 2H), 2.50 (overlapped, 3H), 1.82 (d, $J = 12.0$ Hz, 2H), 1.62 (br, 1H), 1.49–1.40 (m, 2H). ^{13}C -NMR (100 MHz, $\text{DMSO}-d_6$): δ 194.1, 164.9, 159.4, 158.6, 145.7, 142.0, 117.6, 116.0, 110.3, 100.5, 65.3, 52.5, 51.6, 36.8, 36.3, 26.4, 18.5. ESI-HRMS: m/z $[\text{M} + \text{H}]^+$ calcd for $\text{C}_{19}\text{H}_{24}\text{NO}_5$ 346.1649, found 346.1651.

3-(3-(4-Methylpiperazin-1-yl)propanoyl)-5-methyl-7-hydroxycoumarin hydrochloride (15). Yellow solid, yield: 31.4%, m.p.: 210–212 °C (decomposed). ^1H -NMR (400 MHz, CF_3COOD): δ 9.07 (s, 1H), 6.92 (s, 1H), 6.81 (s, 1H), 4.22 (d, $J = 8.0$ Hz, 2H), 4.12–3.90 (m, 10H), 3.16 (s, 3H), 2.61 (s, 3H). ^{13}C -NMR (100 MHz, CF_3COOD): δ 197.0, 164.4, 158.8, 149.6, 144.2, 116.8, 116.3, 115.3, 115.2, 112.2, 101.0, 53.9, 51.1, 50.0, 43.4, 16.5. ESI-HRMS: m/z $[\text{M} + \text{H}]^+$ calcd for $\text{C}_{18}\text{H}_{23}\text{N}_2\text{O}_4$ 331.1652, found 331.1657.

3-(3-(4-Phenylpiperazin-1-yl)propanoyl)-5-methyl-7-hydroxycoumarin hydrochloride (16). Yellow solid, yield: 21.1%, m.p.: 230–231 °C (decomposed). ^1H -NMR (400 MHz, $\text{DMSO}-d_6$): δ 11.35 (br, D_2O exchangeable, 1H), 10.69 (br, D_2O exchangeable, 1H), 8.63 (s, 1H), 7.26 (t, $J = 8.8$ Hz, 2H), 7.00 (d, $J = 8.8$ Hz, 2H), 6.88–6.84 (m, 1H), 6.78–6.77 (m, 1H), 6.68–6.67 (m, 1H), 3.81 (br, 2H), 3.64 (t, $J = 7.2$ Hz, 2H), 3.57 (br, 2H), 3.48 (t, $J = 7.2$ Hz, 2H), 3.16 (br, 4H), 2.51 (overlapped, 3H). ^{13}C -NMR (150 MHz, $\text{DMSO}-d_6$): δ 193.7, 164.6, 159.0, 158.3, 149.6, 145.3, 141.7, 129.2, 120.1, 117.2, 116.0, 115.6, 109.9, 100.1, 51.2, 50.8, 45.6, 36.4, 18.1. ESI-HRMS: m/z $[\text{M} + \text{H}]^+$ calcd for $\text{C}_{23}\text{H}_{25}\text{N}_2\text{O}_4$ 393.1809, found 393.1803.

3-(3-(4-(2-Fluorophenyl) piperazin-1-yl) propanoyl)-5-methyl-7-hydroxycoumarin hydrochloride (17). Yellow solid, yield: 39.4%, m.p.: 233–235 °C (decomposed). ^1H -NMR (400 MHz, $\text{DMSO}-d_6$): δ 8.54 (s, 1H), 6.92–7.14 (m, 4H), 6.72 (d, $J = 2.0$ Hz, 1H), 6.60 (d, $J = 2.0$ Hz, 1H), 3.24 (t, $J = 7.1$ Hz, 2H), 3.00 (br, 4H),

2.75 (t, $J = 7.1$ Hz, 2H), 2.61 (br, 4H), 2.49 (s, 3H). ^{13}C -NMR (100 MHz, $\text{DMSO}-d_6$): δ 196.2, 164.1, 159.0, 158.0, 156.1, 153.7, 144.5, 141.3, 139.7, 124.8, 122.3, 119.2, 118.0, 116.0, 115.8, 115.4, 109.8, 99.9, 52.6, 49.9, 18.0. ESI-HRMS: m/z $[\text{M} + \text{H}]^+$ calcd for $\text{C}_{23}\text{H}_{24}\text{FN}_2\text{O}_4$ 411.1715, found 411.1715.

3-(3-(4-(Tetrahydrofuran-3-carbonyl)piperazin-1-yl) propanoyl)-5-methyl-7-hydroxycoumarin hydrochloride (18). Yellow solid, yield: 45.5%, m.p.: 241–243 °C (decomposed). ^1H -NMR (400 MHz, D_2O): δ 8.67 (s, 1H), 6.70 (s, 1H), 6.54 (s, 1H), 3.99–3.94 (m, 6H), 3.62–3.50 (m, 8H), 2.45 (s, 3H), 2.40–2.31 (br, 1H), 1.97 (s, 4H). ^{13}C -NMR (100 MHz, $\text{DMSO}-d_6$): δ 193.5, 169.5, 164.5, 158.9, 158.2, 145.3, 141.6, 117.1, 115.5, 109.8, 100.0, 75.0, 68.3, 50.8, 41.7, 38.4, 36.2, 27.8, 25.2, 18.0. ESI-HRMS: m/z $[\text{M} + \text{H}]^+$ calcd for $\text{C}_{22}\text{H}_{27}\text{N}_2\text{O}_6$ 415.1864, found 415.1867.

The general procedure for the preparation of target compounds 19–29 is described below.

A secondary alkyl amine (20.0 mmol, 10 equiv.) was added to a stirred suspension of PFA (0.61 g, 10.0 mmol, 5 equiv.) in ethanol (25 mL). After 2 h of reflux at 78 °C, a coumarin intermediate (2.0 mmol, 1 equiv.) was added, and the reaction mixture was refluxed at 78 °C for 4–8 h and monitored with TLC. Subsequently, the mixture was cooled to room temperature and filtered to obtain a yellow solid. The residue was washed with ethanol or methanol to obtain a pure product.

3-Acetyl-8-(piperidyl methyl)-7-hydroxycoumarin (19). Yellow solid, yield: 48.2%, m.p.: 231–233 °C (decomposed). ^1H -NMR (400 MHz, $\text{DMSO}-d_6$): δ 8.42 (s, 1H), 7.55 (d, $J = 8.9$ Hz, 1H), 6.50 (d, $J = 8.9$ Hz, 1H), 4.08 (s, 2H), 2.89–2.87 (m, 4H), 2.50 (s, 3H), 1.67–1.62 (m, 4H), 1.52–1.48 (m, 2H). ^{13}C -NMR (125 MHz, $\text{DMSO}-d_6$): δ 194.0, 173.1, 159.7, 156.7, 147.6, 132.1, 117.7, 112.8, 107.5, 104.6, 52.3, 51.9, 30.1, 23.8, 22.2. ESI-HRMS: m/z $[\text{M} + \text{H}]^+$ calcd for $\text{C}_{17}\text{H}_{20}\text{NO}_4$ 302.1387, found 302.1389.

3-Acetyl-8-(diethylamino methyl)-7-hydroxycoumarin (20). Yellow solid, yield: 18.1%, m.p.: 221–223 °C (decomposed). ^1H -NMR (400 MHz, $\text{DMSO}-d_6$): δ 8.39 (s, 1H), 7.50 (d, $J = 8.9$ Hz, 1H), 6.41 (d, $J = 8.9$ Hz, 1H), 4.15 (s, 2H), 2.94 (q, $J = 7.2$ Hz, 4H), 2.48 (s, 3H), 1.20 (t, $J = 7.2$ Hz, 6H). ^{13}C -NMR (125 MHz, $\text{DMSO}-d_6$): δ 193.9, 175.1, 159.9, 157.0, 147.4, 132.3, 118.4, 111.5, 106.8, 104.4, 47.5, 46.4, 30.1, 9.5. ESI-HRMS: m/z $[\text{M} + \text{H}]^+$ calcd for $\text{C}_{16}\text{H}_{20}\text{NO}_4$ 290.1387, found 290.1385.

3-Acetyl-8-(3-diethylamino methyl)-5-methyl-7-hydroxycoumarin hydrochloride (21). Yellow solid, yield: 20.2%, m.p.: 225–227 °C (decomposed). ^1H -NMR (400 MHz, $\text{DMSO}-d_6$): δ 8.37 (s, 1H), 6.28 (s, 1H), 4.12 (s, 2H), 2.96 (q, $J = 7.2$ Hz, 4H), 2.48 (s, 3H), 2.33 (s, 3H), 1.20 (t, $J = 7.2$ Hz, 6H). ^{13}C -NMR (125 MHz, $\text{DMSO}-d_6$): δ 193.8, 175.6, 159.9, 158.0, 143.7, 140.0, 119.7, 109.8, 106.3, 102.6, 47.3, 46.4, 30.1, 17.9, 9.4. ESI-HRMS: m/z $[\text{M} + \text{H}]^+$ calcd for $\text{C}_{17}\text{H}_{22}\text{NO}_4$ 304.1543, found 304.1546.

3-Acetyl-8-(3-piperidyl methyl)-5-methyl-7-hydroxycoumarin hydrochloride (22). Yellow solid, yield: 75.5%, m.p.: 234–235 °C (decomposed). ^1H -NMR (400 MHz, $\text{DMSO}-d_6$): δ 8.39 (s, 1H), 6.36 (s, 1H), 4.05 (s, 2H), 2.90 (t, $J = 5.0$ Hz, 4H), 2.49 (s, 3H), 2.35 (s, 3H), 1.66–1.65 (m, 4H), 1.50–1.49 (m, 2H). ^{13}C -NMR (125 MHz, $\text{DMSO}-d_6$): δ 193.9, 173.5, 159.8, 157.7, 143.9, 139.9, 118.9, 111.2, 106.9, 102.8, 52.2, 51.7, 30.1, 23.7, 22.1, 17.9. ESI-HRMS: m/z $[\text{M} + \text{H}]^+$ calcd for $\text{C}_{18}\text{H}_{22}\text{NO}_4$ 316.1543, found 316.1537.

3-Acetyl-8-(morpholinyl methyl)-5-methyl-7-hydroxycoumarin hydrochloride (23). Yellow solid, yield: 71.1%, m.p.: 231–233 °C (decomposed). ¹H-NMR (400 MHz, DMSO-*d*₆): δ 8.52 (s, 1H), 6.68 (s, 1H), 3.86 (s, 2H), 3.61 (t, *J* = 4.2 Hz, 4H), 2.59 (t, *J* = 4.2 Hz, 4H), 2.55 (s, 3H), 2.46 (s, 3H). ¹³C-NMR (125 MHz, DMSO-*d*₆): δ 194.6, 165.2, 158.9, 156.1, 144.7, 140.0, 116.9, 115.6, 109.3, 105.6, 65.8, 52.4, 51.3, 30.1, 17.9. ESI-HRMS: *m/z* [M + H]⁺ calcd for C₁₇H₂₀NO₅ 318.1336, found 318.1342.

3-Acetyl-8-(4-hydroxypiperidin-1-yl methyl)-5-methyl-7-hydroxycoumarin hydrochloride (24). Yellow solid, yield: 51.2%, m.p.: 210–211 °C (decomposed). ¹H-NMR (500 MHz, D₂O and CF₃COOD) δ 8.30 (s, 1H), 6.61 (s, 1H), 4.11 (d, *J* = 5.2 Hz, 2H), 3.92–3.68 (m, 1H), 3.38 (d, *J* = 12.2 Hz, 1H), 3.17 (s, 2H), 2.99–2.93 (m, 1H), 2.33 (s, 3H), 2.21 (s, 3H), 1.95 (d, *J* = 13.5 Hz, 1H), 1.76 (s, 2H), 1.56–1.47 (m, 1H). ¹³C-NMR (100 MHz, D₂O and CF₃COOD) δ 199.3, 163.2, 159.6, 156.3, 146.6, 144.4, 117.2, 114.9, 110.3, 100.9, 64.4, 60.5, 51.0, 47.7, 30.5, 28.8, 28.6, 17.5. ESI-HRMS: *m/z* [M + H]⁺ calcd for C₁₈H₂₂NO₅ 332.1492, found 332.1495.

3-Acetyl-8-((4-(hydroxymethyl)piperidin-1-yl)methyl)-5-methyl-7-hydroxycoumarin hydrochloride (25). Yellow solid, yield: 55.3%, m.p.: 211–213 °C (decomposed). ¹H-NMR (400 MHz, DMSO-*d*₆): δ 8.41 (s, 1H), 6.37 (s, 1H), 4.08 (s, 2H), 3.27 (d, *J* = 6.2 Hz, 2H), 3.17 (d, *J* = 11.8 Hz, 2H), 2.67 (t, *J* = 11.2 Hz, 2H), 2.50 (overlapped, 3H), 2.37 (s, 3H), 1.76 (d, *J* = 12.0 Hz, 2H), 1.55 (br, 1H), 1.35–1.24 (m, 2H). ¹³C-NMR (125 MHz, D₂O and CF₃COOD): δ 202.9, 164.7, 160.7, 160.4, 158.2, 150.5, 148.1, 119.1, 117.4, 113.2, 102.1, 71.8, 54.7, 51.3, 34.0, 27.0, 18.4. ESI-HRMS: *m/z* [M + H]⁺ calcd for C₁₉H₂₄NO₅ 346.1649, found 346.1653.

3-Acetyl-8-((4-methylpiperazin-1-yl)methyl)-5-methyl-7-hydroxycoumarin hydrochloride (26). Yellow solid, yield: 42.2%, m.p.: 220–223 °C (decomposed). ¹H-NMR (400 MHz, D₂O): δ 8.82 (s, 1H), 6.96 (s, 1H), 4.63 (s, 2H), 3.76–3.68 (br, 8H), 3.03 (s, 3H), 2.67 (s, 3H), 2.58 (s, 3H). ¹³C-NMR (125 MHz, D₂O): δ 199.3, 163.4, 160.5, 156.9, 147.6, 145.1, 117.8, 115.1, 110.9, 50.4, 50.1, 48.8, 48.6, 42.9, 29.1, 17.9. ESI-HRMS: *m/z* [M + H]⁺ calcd for C₁₈H₂₃N₂O₄ 331.1652, found 331.1658.

3-Acetyl-8-((4-phenylpiperazin-1-yl)methyl)-5-methyl-7-hydroxycoumarin hydrochloride (27). Yellow solid, yield: 56.4%, m.p.: 245–247 °C (decomposed). ¹H-NMR (400 MHz, DMSO-*d*₆): δ 8.53 (s, 1H), 7.21 (t, *J* = 8.3 Hz, 2H), 6.94 (d, *J* = 8.2 Hz, 2H), 6.79 (t, *J* = 7.2 Hz, 1H), 6.68 (s, 1H), 3.97 (s, 2H), 3.22–3.15 (br, 4H), 2.92–2.74 (br, 4H), 2.55 (s, 3H), 2.47 (s, 3H). ¹³C-NMR (100 MHz, DMSO-*d*₆): δ 194.5, 165.8, 159.0, 156.1, 150.6, 144.7, 140.1, 129.0, 119.2, 116.6, 115.8, 115.6, 109.2, 105.5, 51.8, 51.0, 47.8, 30.1, 17.9. ESI-HRMS: *m/z* [M + H]⁺ calcd for C₂₃H₂₅N₂O₄ 393.1809, found 393.1806.

3-Acetyl-8-((4-(2-fluorophenyl)piperazin-1-yl)methyl)-5-methyl-7-hydroxycoumarin hydrochloride (28). Yellow solid, yield: 51.4%, m.p.: 251–253 °C (decomposed). ¹H-NMR (500 MHz, DMSO-*d*₆): δ 8.55 (s, 1H), 7.16–6.96 (m, 4H), 6.70 (s, 1H), 3.99 (s, 2H), 3.08 (s, 4H), 2.81 (s, 4H), 2.56 (s, 3H), 2.48 (s, 3H). ¹³C-NMR (100 MHz, CDCl₃) δ 195.9, 165.6, 159.9, 157.1, 156.0, 154.6, 145.7, 140.4, 139.4, 139.4, 124.7, 124.7, 123.3, 123.2, 119.2, 119.2, 118.1, 116.5, 116.3, 116.3, 110.5, 104.9, 53.8, 52.8, 50.3, 30.8, 18.6. ESI-HRMS: *m/z* [M + H]⁺ calcd for C₂₃H₂₄FN₂O₄ 411.1715, found 411.1707.

3-Acetyl-8-(3-(4-(tetrahydrofuran-3-carbonyl)piperazin-1-yl)methyl)-5-methyl-7-hydroxycoumarin hydrochloride (29). Yellow solid, yield: 41.4%, m.p.: 222–224 °C (decomposed). ¹H-NMR (400 MHz, DMSO-*d*₆): δ 8.53 (s, 1H), 6.71 (s, 1H), 4.65–4.63 (m, 1H), 3.84 (s, 2H), 3.79–3.67 (m, 2H), 3.63–3.39 (m, 4H), 2.62–2.52 (overlapped, 7H), 2.48 (s, 3H), 2.06–1.92 (m, 2H), 1.96–1.75 (m, 2H). ¹³C-NMR (125 MHz, D₂O): δ 198.9, 173.3, 164.4, 160.2, 156.8, 147.2, 144.6, 117.0, 115.4, 110.5, 100.4, 75.0, 69.5, 51.0, 48.4, 41.7, 38.8, 29.4, 25.1, 17.7. ESI-HRMS: *m/z* [M + H]⁺ calcd. for C₂₂H₂₇N₂O₆ 415.1864, found 415.1865.

Biology

NO inhibition assay. Murine RAW264.7 macrophages were obtained from the Institute of Basic Medical Sciences, Chinese Academy of Medical Sciences and Peking Union Medical College. The experiment was carried out following the protocol in a previous report.⁵¹ We cultured the RAW264.7 cells in Dulbecco's modified Eagle medium (DMEM; #12100-500, Solarbio, Beijing, China) supplemented with 10% fetal bovine serum (FBS; #11011-8611, Sijiqing, Hangzhou, China) in a 5% CO₂ atmosphere and 100% relative humidity at 37 °C. The cells were seeded into 96-well plates for 24 h at a cell concentration of 1.5 × 10⁴ cells (100 μL) per well. Then, the screened compounds at 1.0 × 10⁻⁵ mol L⁻¹ and curcumin (1.0 × 10⁻⁵ mol L⁻¹) as a positive control were dissolved in dimethyl sulfoxide (DMSO; #0231, Amresco, USA) and added to the plates. After 1 h, the cells were treated with LPS (500 ng mL⁻¹, #L4391, Sigma, USA), and incubation was continued for an additional 24 h. The supernatant of the culture medium was collected (100 μL), and the NO₂⁻ concentration was detected using an equal volume of Griess reagent to determine the NO concentration. The optical density (OD) values were measured at 540 nm on a microplate reader (BioTek H1, Winooski, VT, USA). The inhibition ratio of NO production was calculated according to eqn (2).

$$\% \text{ inhibition} = \frac{\text{OD}_{\text{model}} - \text{OD}_{\text{test}}}{\text{OD}_{\text{model}} - \text{OD}_{\text{control}}} \times 100\% \quad (2)$$

where OD_{model} is the OD value of the model group (LPS), OD_{test} is the OD value of the test group (LPS and test compounds), and OD_{control} is the OD value of the control group (untreated).

TNF-α inhibition assay

The level of TNF-α was measured using ELISA kits (#88732422, Thermo Fisher, USA). The specific procedure followed the protocol in a previous report.⁵² RAW264.7 cells were obtained from the American Type Culture Collection (Rockville, MD, USA) and grown in RPMI-1640 culture medium (#12633012, Thermo Fisher, USA) supplemented with 10% FBS (#10099, Thermo Fisher, USA) in a 5% CO₂ atmosphere at 37 °C. When the confluence reached approximately 80%, the cells were seeded into 96-well plates at a concentration of 2.0 × 10⁴ cells (100 μL) per well and incubated for 12–18 h under 5% CO₂. The supernatant was discarded, and the cells were cultured with 2% FBS for 4 h. Then, 1.0 × 10⁻⁵ mol L⁻¹ screened compounds and dexamethasone as a positive control dissolved in DMSO (#67685, Sigma, USA) were added to the plates, and

the cells were incubated for 1 h. LPS ($1 \mu\text{g mL}^{-1}$) was supplemented for an additional 24 h. The supernatant of the culture medium was collected to detect TNF- α release. The OD values were measured at 450 nm and 570 nm on a microplate reader. The TNF- α concentrations after treatment with the screened compounds were obtained with a standard curve. The inhibition ratio of TNF- α was calculated based on eqn (3).

$$\% \text{ inhibition} = \frac{C_{\text{model}} - C_{\text{test}}}{C_{\text{model}}} \quad (3)$$

where C_{model} is the TNF- α concentration of the model group (LPS), C_{test} is the TNF- α concentration of the test group (LPS and test compounds), and C_{control} is the TNF- α concentration of the control group (untreated).

Calculation details

Primary conformations were obtained by using the MOE package⁵³ with the MMFF94 molecular mechanics force field. The geometries of the initial conformations were optimized using Gaussian 16 software⁵⁴ at the level of B3LYP/6-311G(d,p), and the polarizable continuum model (PCM)^{55,56} was employed to simulate the solvation effects in ethanol. VDD atomic charges were calculated by using the wave function analysis software Multiwfn.⁵⁷ The atomic densities were analysed by employing the built-in sphericalized atomic densities in free states.

Conflicts of interest

There are no conflicts to declare.

Acknowledgements

We gratefully acknowledge the CAMS Innovation Fund for Medical Sciences (CIFMS, No. 2016-I2M-3-009) and the Drug Innovation Major Project (2018ZX09711-001-005) for providing financial support for this work.

Notes and references

- Q. Yang and J. Zhou, *Glia*, 2019, **67**, 1017–1035.
- E. Danelius, R. G. Ohm, Ahsanullah, M. Mulumba, H. Ong, S. Chemtob, M. Erdelyi and W. D. Lubell, *J. Med. Chem.*, 2019, **62**, 11071–11079.
- Y. V. Perfilyeva, N. Abdolla, Y. O. Ostapchuk, R. Tleulieva, V. C. Krasnoshtanov, A. V. Perfilyeva and N. N. Belyaev, *Inflammation*, 2019, **42**, 276–289.
- P. La Vitola, C. Balducci, M. Baroni, L. Artioli, G. Santamaria, M. Castiglioni, M. Cerovic, L. Colombo, L. Caldinelli and L. Pollegioni, *Neuropathol. Appl. Neurobiol.*, 2021, **47**, 43–60.
- M. K. Demoruelle, T. M. Wilson and K. D. Deane, *Immunol. Rev.*, 2020, **294**, 124–132.
- D. A. Sliter, J. Martinez, L. Hao, X. Chen, N. Sun, T. D. Fischer, J. L. Burman, Y. Li, Z. Zhang and D. P. Narendra, *Nature*, 2018, **561**, 258–262.
- (a) C. Lino, M. Taveira, G. Viana and F. Matos, *Phytother. Res.*, 1997, **11**, 211–215; (b) A. M. Mahmoud, W. G. Hozayen, I. H. Hasan, E. Shaban and M. Bin-Jumah, *Inflammation*, 2019, **42**, 1103–1116.
- Z. Xiao, D. Chen, S. Song, R. van der Vlag, P. E. van der Wouden, R. van Merkerk, R. H. Cool, A. K. Hirsch, B. N. Melgert and W. J. Quax, *J. Med. Chem.*, 2020, **63**, 11920–11933.
- S. Abrahams, W. L. Haylett, G. Johnson, J. A. Carr and S. Bardien, *Neuroscience*, 2019, **406**, 1–21.
- Z. Cournia, L. Leng, S. Gandavadi, X. Du, R. Bucala and W. L. Jorgensen, *J. Med. Chem.*, 2009, **52**, 416–424.
- J. Garai and T. Lóránd, *Curr. Med. Chem.*, 2009, **16**, 1091–1114.
- H. Y. Bae, M. J. Kim, J. H. Sim and C. E. Song, *Angew. Chem., Int. Ed.*, 2016, **55**, 10825–10829.
- J. Guang, S. Rout, M. Bihani, A. J. Larson, H. D. Arman and J. C.-G. Zhao, *Org. Lett.*, 2016, **18**, 2648–2651.
- H. Jo, A. H. Hassan, S. Y. Jung, J. K. Lee, Y. S. Cho and S.-J. Min, *Org. Lett.*, 2018, **20**, 1175–1178.
- (a) Y. Zhang, Y.-Z. Zhan, Y. Ma, X.-W. Hua, W. Wei, X. Zhang, H.-B. Song, Z.-M. Li and B.-L. Wang, *Chin. Chem. Lett.*, 2018, **29**, 441–446; (b) Y. Zhang, X.-H. Liu, Y.-Z. Zhan, L.-Y. Zhang, Z.-M. Li, Y.-H. Li, X. Zhang and B.-L. Wang, *Bioorg. Med. Chem. Lett.*, 2016, **26**, 4661–4665.
- B. Biersack, K. Ahmed, S. Padhye and R. Schobert, *Expert Opin. Drug Discovery*, 2018, **13**, 39–49.
- D. Tao, Y. Wang, X.-Q. Bao, B.-B. Yang, F. Gao, L. Wang, D. Zhang and L. Li, *Eur. J. Med. Chem.*, 2019, **173**, 203–212.
- D. M. Perrine, N. R. Sabanayagam and K. J. Reynolds, *J. Chem. Educ.*, 1998, **75**, 1266.
- F. A. Davis, N. Theddu and P. M. Gaspari, *Org. Lett.*, 2009, **11**, 1647–1650.
- (a) M. Betti, *Gazz. Chim. Ital.*, 1900, **30**, 301M–309M; (b) M. Betti, *Gazz. Chim. Ital.*, 1900, **30**, 310–316; (c) M. Betti, *Gazz. Chim. Ital.*, 1906, **36**, 392–394.
- R. Ding, Z. A. De los Santos and C. Wolf, *ACS Catal.*, 2019, **9**, 2169–2176.
- A. Gangopadhyay and A. K. Mahapatra, *New J. Chem.*, 2019, **43**, 11743–11748.
- J. L. Andersen, T. J. Schröder, S. Christensen, D. Strandbygård, L. T. Pallesen, M. M. García-Alai, S. Lindberg, M. Langgård, J. C. Eskildsen and L. David, *Acta Crystallogr., Sect. D: Biol. Crystallogr.*, 2014, **70**, 451–460.
- T. Goto, H. Kajiwara, M. Yoshinari, E. Fukuhara, S. Kobayashi and T. Tanaka, *Biomaterials*, 2003, **24**, 3885–3892.
- C. A. Kontogiorgis and D. J. Hadjipavlou-Litina, *J. Med. Chem.*, 2005, **48**, 6400–6408.
- A. Avcı, H. Taşci, Ü. Kandemir, Ö. D. Can, N. Gökhan-Kelekçi and B. Tozkoparan, *Bioorg. Chem.*, 2020, **100**, 103892.
- A. Mehmood, S. I. Jones, P. Tao and B. G. Janesko, *J. Chem. Inf. Model.*, 2018, **58**, 1836–1846.
- C. Fonseca Guerra, J. W. Handgraaf, E. J. Baerends and F. M. Bickelhaupt, *J. Comput. Chem.*, 2004, **25**, 189–210.

- 29 P. Politzer, J. S. Murray and F. A. Bulat, *J. Mol. Model.*, 2010, **16**, 1731–1742.
- 30 R. Flores-Moreno, *J. Chem. Theory Comput.*, 2010, **6**, 48–54.
- 31 M. Franco-Pérez, P. W. Ayers, J. L. Gázquez and A. Vela, *Phys. Chem. Chem. Phys.*, 2017, **19**, 13687–13695.
- 32 T. F. Cummings and J. R. Shelton, *J. Org. Chem.*, 1960, **25**, 419–423.
- 33 C. S. Graebin, F. V. Ribeiro, K. R. Rogério and A. E. Kümmerle, *Curr. Org. Synth.*, 2019, **16**, 855–899.
- 34 M. O. Ratnikov and M. P. Doyle, *J. Am. Chem. Soc.*, 2013, **135**, 1549–1557.
- 35 C. Cardellicchio, M. A. M. Capozzi and F. Naso, *Tetrahedron: Asymmetry*, 2010, **21**, 507–517.
- 36 S. D. Dindulkar, V. G. Puranik and Y. T. Jeong, *Tetrahedron Lett.*, 2012, **53**, 4376–4380.
- 37 T. Lu and F.-W. Chen, *Acta Phys.-Chim. Sin.*, 2012, **28**, 1–18.
- 38 J. Cao, Q. Ren, F. Chen and T. Lu, *Sci. China: Chem.*, 2015, **58**, 1845–1852.
- 39 B. Wang, C. Rong, P. K. Chattaraj and S. Liu, *Theor. Chem. Acc.*, 2019, **138**, 1–9.
- 40 F. M. Bickelhaupt, N. J. van Eikema Hommes, C. Fonseca Guerra and E. J. Baerends, *Organometallics*, 1996, **15**, 2923–2931.
- 41 M. N. C. Zarycz and C. I. Fonseca Guerra, *J. Phys. Chem. Lett.*, 2018, **9**, 3720–3724.
- 42 G. Fraenkel, R. E. Carter, A. McLachlan and J. H. Richards, *J. Am. Chem. Soc.*, 1960, **82**, 5846–5850.
- 43 H. Neuvonen, K. Neuvonen, A. Koch, E. Kleinpeter and P. Pasanen, *J. Org. Chem.*, 2002, **67**, 6995–7003.
- 44 A. Zheng, M. Yang, Y. Yue, C. Ye and F. Deng, *Chem. Phys. Lett.*, 2004, **399**, 172–176.
- 45 (a) J. L. Jeffrey, F. R. Petronijević and D. W. MacMillan, *J. Am. Chem. Soc.*, 2015, **137**, 8404–8407; (b) S. Faizi, T. Sarfaraz, S. Sumbul, A. Jabeen, S. A. Halim, M. A. Mesaik and Z. Ul-Haq, *Med. Chem.*, 2020, **16**, 531–543.
- 46 M. Garazd, Y. L. Garazd, S. Shilin and V. Khilya, *Chem. Nat. Compd.*, 2000, **36**, 485–492.
- 47 H. Mostafavi, R. Najjar and E. Maskani, *Chem. Nat. Compd.*, 2013, **49**, 423–425.
- 48 R. Desai, *J. Org. Chem.*, 1961, **26**, 5251–5253.
- 49 N. Liang, Y. Sang, W. Liu, W. Yu and X. Wang, *Inflammation*, 2018, **41**, 835–845.
- 50 (a) J. Liu, D. Zhang, M. Zhang, J. Zhao, R. Chen, N. Wang, D. Zhang and J. Dai, *J. Nat. Prod.*, 2016, **79**, 2229–2235; (b) T. Esatbeyoglu, P. Huebbe, M. A. Insa, E. DawnChin, A. E. Wagner and G. Rimbach, *Angew. Chem., Int. Ed.*, 2012, **51**, 5308–5332; (c) P. Basnet and N. Skalko-Basnet, *Molecules*, 2011, **16**, 4567–4598.
- 51 B. Li, S. Cai, Y.-A. Yang, S.-C. Chen, R. Chen, J.-B. Shi, X.-H. Liu and W.-J. Tang, *Eur. J. Med. Chem.*, 2017, **139**, 337–348.
- 52 Z. Liu, L. Tang, H. Zhu, T. Xu, C. Qiu, S. Zheng, Y. Gu, J. Feng, Y. Zhang and G. Liang, *J. Med. Chem.*, 2016, **59**, 4637–4650.
- 53 MOE2009.10, Chemical Computing Group Inc.
- 54 M. J. Frisch, G. W. Trucks, H. B. Schlegel, G. E. Scuseria, M. A. Robb, J. R. Cheeseman, G. Scalmani, V. Barone, G. A. Petersson, H. Nakatsuji, X. Li, M. Caricato, A. V. Marenich, J. Bloino, B. G. Janesko, R. Gomperts, B. Mennucci, H. P. Hratchian, J. V. Ortiz, A. F. Izmaylov, J. L. Sonnenberg, D. Williams-Young, F. Ding, F. Lipparini, F. Egidi, J. Goings, B. Peng, A. Petrone, T. Henderson, D. Ranasinghe, V. G. Zakrzewski, J. Gao, N. Rega, G. Zheng, W. Liang, M. Hada, M. Ehara, K. Toyota, R. Fukuda, J. Hasegawa, M. Ishida, T. Nakajima, Y. Honda, O. Kitao, H. Nakai, T. Vreven, K. Throssell, J. A. Montgomery, Jr., J. E. Peralta, F. Ogliaro, M. J. Bearpark, J. J. Heyd, E. N. Brothers, K. N. Kudin, V. N. Staroverov, T. A. Keith, R. Kobayashi, J. Normand, K. Raghavachari, A. P. Rendell, J. C. Burant, S. S. Iyengar, J. Tomasi, M. Cossi, J. M. Millam, M. Klene, C. Adamo, R. Cammi, J. W. Ochterski, R. L. Martin, K. Morokuma, O. Farkas, J. B. Foresman and D. J. Fox, *Gaussian 16, Revision B.01*, Gaussian, Inc., Wallingford CT, 2016.
- 55 A. V. Marenich, C. J. Cramer and D. G. Truhlar, *J. Phys. Chem. B*, 2009, **113**, 6378–6396.
- 56 K. Begam, S. Bhandari, B. Maiti and B. D. Dunietz, *J. Chem. Theory Comput.*, 2020, **16**, 3287–3293.
- 57 (a) Multiwfn website available from: <http://Multiwfn.codeplex.com>; (b) T. Lu and F. Chen, *J. Comput. Chem.*, 2012, **33**, 580–592.